

Heat-Mechanics Interaction Behavior of Lead Rubber Bearings for Seismic Base Isolation under Large and Cyclic Lateral Deformation

Part 1: Dynamic Loading Test of LRB and Development of Analytical Method

Akihiro Kondo^a, Yasuo Takenaka^a, Eiji Takaoka^a,
Makiko Hikita^a, Yo Hyodo^a, Haruyuki Kitamura^b

^aKajima Corporation, Tokyo, Japan, e-mail:kondo-akihiro@kajima.com

^bTokyo University of Science, Chiba, Japan

Keywords: Seismic Isolation Structure, Lead Rubber Bearings, Dynamic Loading Tests, Full-scale Specimen, Heat Conduction Analysis, Earthquake Response Analysis

1 ABSTRACT

This paper describes experimental results and derivations of analytical methods for determining the heat-mechanics interaction of an LRB under a large and cyclic lateral deformation. In the experimental stage, dynamic loading tests were conducted for sinusoidal waves and earthquake response waves using full-scale devices and 1/2 and 1/4 reduced models to clarify the scale effect of heat-mechanics interaction behavior.

In the analytical stage, an analytical method was developed to simulate changes in the mechanical properties of the LRB during a cyclic loading test. An earthquake response analysis method was also developed to evaluate the effects of deterioration of damping characteristics of the LRB on base-isolated building responses. Examples of the analysis showed that the changes in the mechanical properties of the lead rubber bearings led to an increase in horizontal displacement of the base-isolated building. The investigations suggest the importance of considering the heat-mechanics interaction behavior of lead rubber bearings.

2 INTRODUCTION

When base-isolated buildings are subjected to long-period strong earthquakes emanating from oceanic trenches, base-isolation devices such as Lead Rubber Bearings (LRB) can be subjected to larger and more cyclic deformations than anticipated in usual structural design.

In an LRB, seismic input energy is absorbed as hysteresis energy of a lead plug, and finally transformed into thermal energy. The resulting large and multiple cyclic deformations of the LRB generate a large amount of heat, causing high temperatures in the lead plug. The resulting deterioration of damping characteristics which encompasses complex thermal and mechanical phenomena can have a serious effect on base-isolated building responses.

However, there is insufficient experimental data on this phenomenon, and no analytical method for evaluating heat-mechanics interaction behavior has been derived. This paper describes experimental results and derivation of analytical methods for determining the heat-mechanics interaction of an LRB under a large and cyclic lateral deformation.

3 EXPERIMENTAL METHODS

3.1 Dynamic loading tests

3.1.1 Specimens

The specimens were full-scale models with a diameter of 1,000 mm and a total rubber thickness of 200 mm,

and 1/2 and 1/4 reduced models. The reduced models were made by scaling down the diameter, the rubber layer thickness and the internal steel plate thickness at the same contraction scale to maintain the thermal capacity and heat transfer properties. The specifications of the specimens are shown in Table 1.

Table 1. List of specimens

Kind of rubber bearing	LRB		
Kind of rubber	Natural rubber G0.4		
Construction scale	Full-Scale LRB1000	Reduced to 1/2 LRB510	Reduced to 1/4 LRB255
Outer diameter D (mm)	1000	510	255
Diameter of lead plug (mm)	200	102	51
Rubber layer thickness t_r (mm)	8	4.08	2.04
Number of rubber layers	25	25	25
Total thickness of rubber h (mm)	200	102	51
Thickness of internal steel plate (mm)	4.3	2.2	1.1
Shape factor ($S=D/4t_r$)	31	31	31
Secondary shape factor ($S_2=D/h$)	5	5	5

3.1.2 Test equipment and measurement items

The loading equipment for reduced models is shown in Figure 1. Items measured were horizontal force, horizontal deformation and specimen temperature. The temperatures of the rubber bearings were measured by thermocouples installed in the specimens. The temperature measurement points in the 1/2-scale LRB specimen are shown in Figure 2 as examples. In the LRB, temperatures were measured at 15 points in total: 3 within the lead plug (P1 to P3), 4 within the rubber at a mid height (RC1 to RC4), 4 within the rubber at a 1/4 height (RQ1 to RQ4), and 4 at the steel flange (MT1 to MT4).

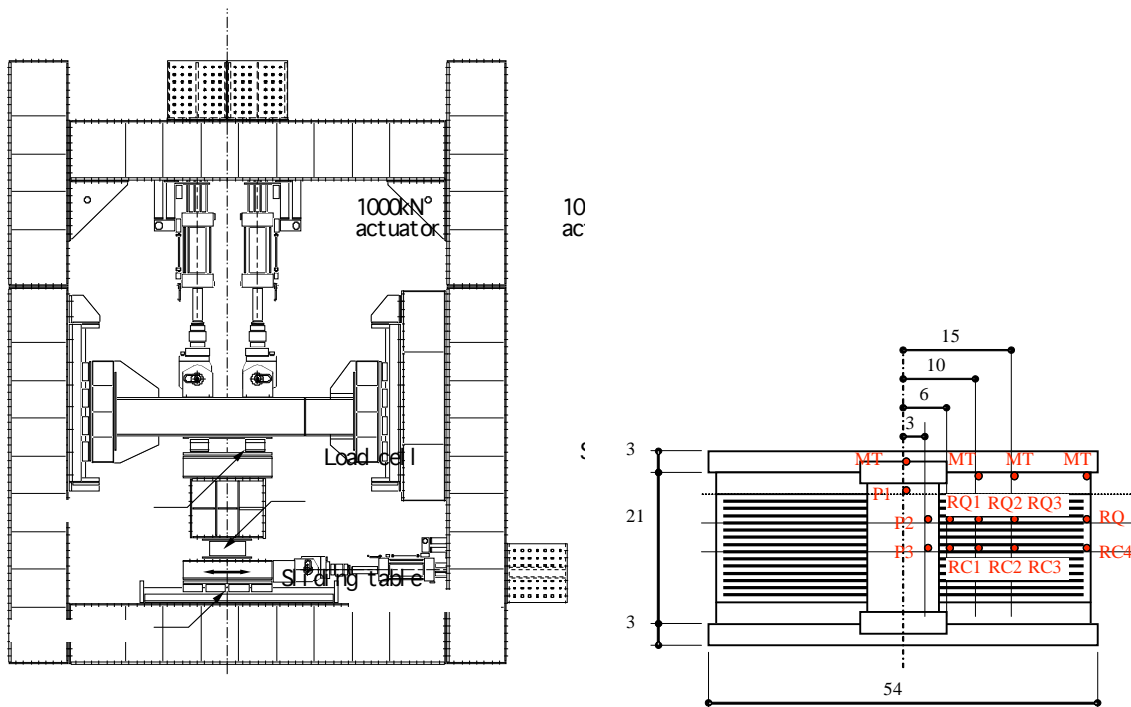


Figure 1. Loading equipment

3.1.3 Loading case for reduced models

Sinusoidal waves and earthquake response waves were applied in the horizontal direction by retaining constant vertical load. The axial stress (vertical load / sectional area of rubber) was set at 3 N/mm² for the full-scale models and 5 N/mm² for the reduced scale models. The parameters of the sine waves were period T, shear strain (horizontal deformation / total rubber thickness), and the number of repetitions. The sine wave cases are listed in Table 2. The earthquake response waves were the response displacement waveforms, which were determined by preliminary earthquake response analyses of a base-isolated building. The earthquake response wave cases are listed in Table 3.

Figure 2. Points of temperature measurement
(1/2 reduced model) LRB510

Table 2. Sine wave cases

Case number	Period T (s)	Shear strain γ (%)	Number of repetition	
			Full-scale model	Reduced model
1	3	50	40	100
2	3	100	20	50
3	3	200	10	100
4	5	100	20	50
5	5	200	10	100

Table 3. Earthquake response wave cases

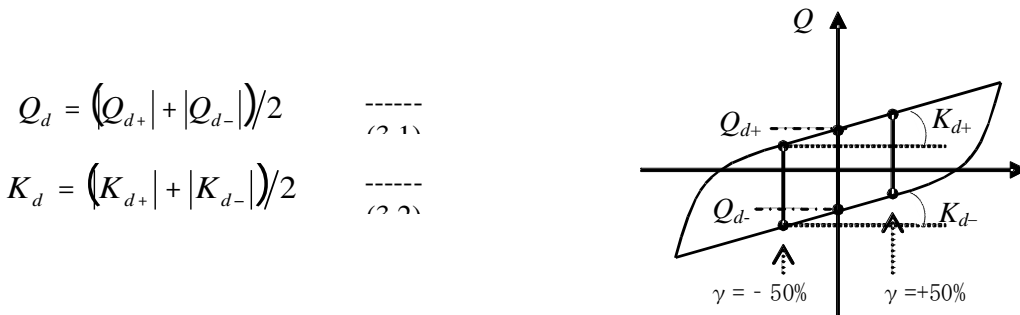
Case number	Name of seismic wave	Max. velocity* (mm/s)	Max. Disp.* (mm)	Max. Shear strain (%)	Total input energy* (kN.m)
6	JMA KOBE 1995 NS	906	284	142	9.97×10^2
7	Knet TOMAKOMAI 2004 NS $\times 1.5$	497	425	213	2.42×10^3
8	MEXICO SCT1 1985 EW	836	325	163	2.51×10^3
9	BCJ-L2	758	428	214	2.61×10^3
10	JSCA KOKUJI	447	232	116	1.32×10^3
11	SANNOMARU EW	711	354	177	3.96×10^3

*Values for at the full-scale model

3.2 Test Results

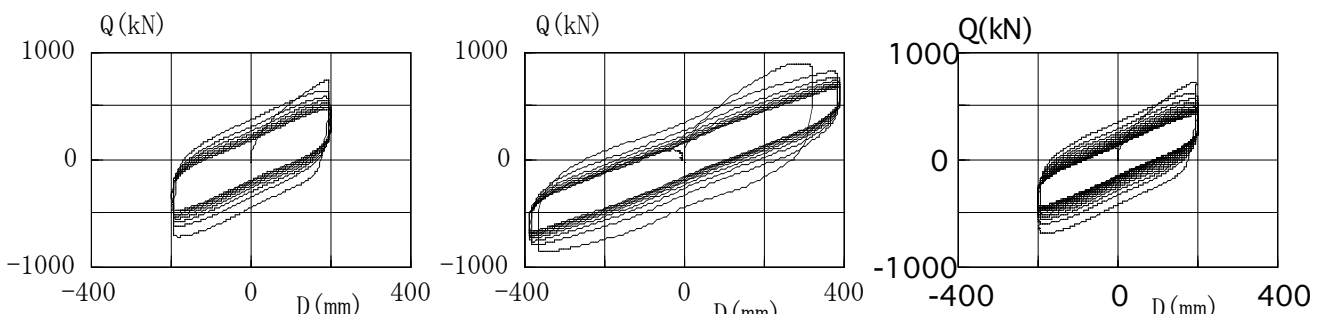
3.2.1 Method for estimating hysteresis characteristics of LRB

Changes in characteristics were estimated based on the yield load Q_d and the stiffness K_d after yielding. Q_d and K_d are given by eq. (3.1) and eq. (3.2). The properties of the rubber bearings were estimated by standardizing the Q_d and K_d values at each cycle.



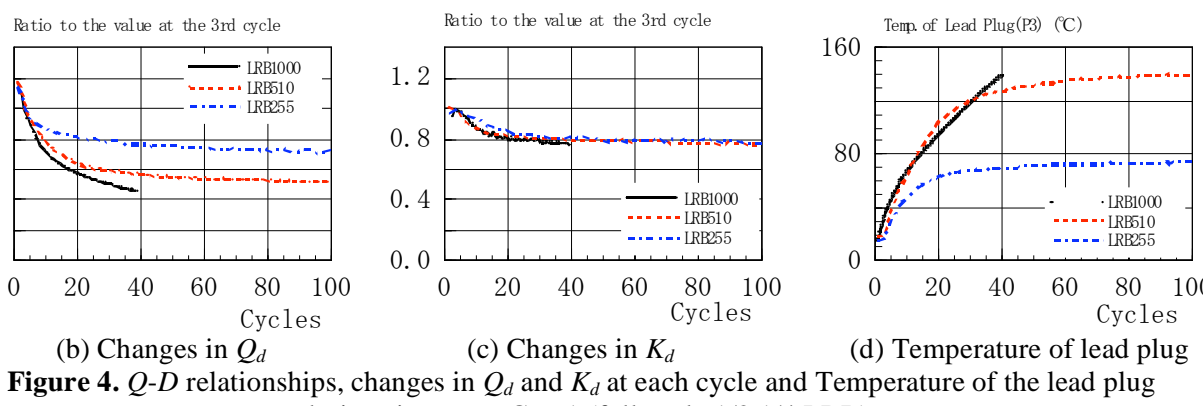
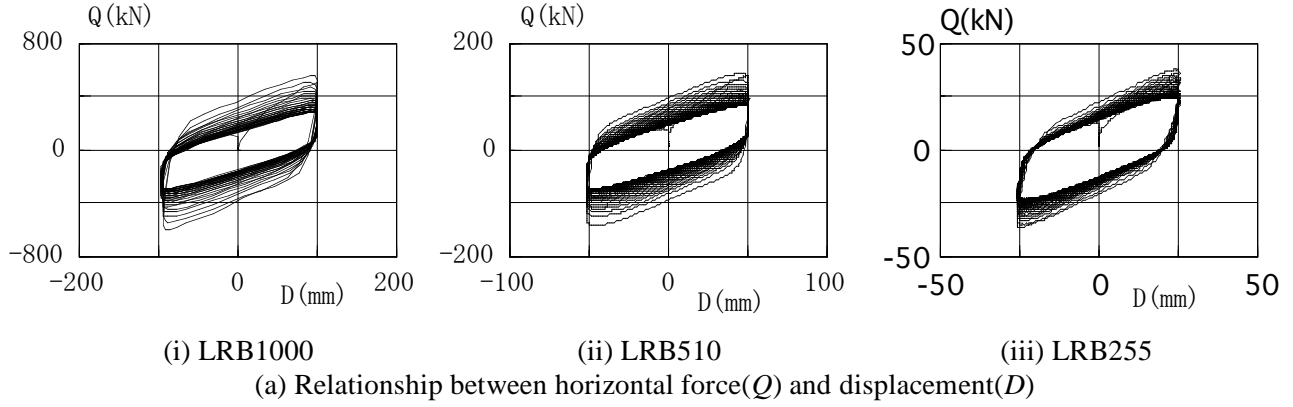
3.2.2 Results of sine wave cases

The relationships between horizontal force Q and horizontal deformation D of the full-scale specimen are shown in Figure 3 for sine wave Case 2 ($T=3$ sec, $\gamma=100\%$), sine wave Case 3 ($T=3$ sec, $\gamma=200\%$), and sine wave Case 4 ($T=5$ sec, $\gamma=100\%$), together with changes in Q_d , K_d and the temperatures of the lead plug (Point P3) at each cycle. Figure 3(a) shows that the shapes of the hysteresis curves were stable but the area surrounded by the curve, which shows the energy absorption amount, decreased as repetition number increased. Figure 3(b) shows that Q_d values started to drop after the start of loading. At the end of loading, the Q_d values became about 45% of those at the third cycle in all cases. However, repetition caused very small changes in K_d values (Figure 3(b)). Figure 3(c) shows that the temperature of the lead plug had reached to about 150°C by the end of loading.



(i) T=3s, $\gamma =100\%$ (Case2) (ii) T=3s, $\gamma =200\%$ (Case3) (iii) T=5s, $\gamma =100\%$ (Case4)
 (a) Relationship between horizontal force(Q) and displacement(D)

(b) Changes in Q_d (c) Changes in K_d (d) Temperature of lead plug
Figure 3. Q - D relationships, changes in Q_d and K_d at each cycle and Temperature of lead plug during sine wave (full-scale LRB)



The results for the full-scale, and the 1/2 and 1/4 reduced specimens are compared in Figure 4 for sine wave Case 1 ($T = 3$ sec, $\gamma = 50\%$). Figure 4(b) shows that the Q_d values for LRB1000 started to drop much more sharply than those of the reduced models. At the end of loading, the Q_d values for LRB1000 became about 45% of those at the third cycle, for LRB500 they become 52%, and for LRB255 they become 73%. However, very small difference was observed between the K_d values for the different sizes (Figure 4(b)). Figure 4(c) shows that the larger the size of the LRB, the larger the rise in temperature of the lead plug.

3.2.3 Results of earthquake response wave cases

The Q - D relationship of the full-scale LRB specimen is shown in Figure 5(a), and changes in Q_d are shown in Figure 5(b) when Sannomaru response waveform was applied. Figure 5(a) shows that the hysteresis curve

was stable but Q_d (the force at $\dot{D} = 0$) tended to decrease with repetition. Figure 5(b) shows a sharp drop at 50 to 120 seconds, which was the principal motion of the San-no-maru response waveform. Changes in temperature of the lead plug are shown in Figure 5(c). The temperature of the lead plug at P3 greatly increased. At 120 seconds, when the principal motion was finished, the temperature reached a ceiling, and it started to drop at about 150 seconds. However, at the other measuring points including the lead plug point P1, it started to increase after the rise at P3. It continued to rise even after 150 seconds when the principal motion finished.

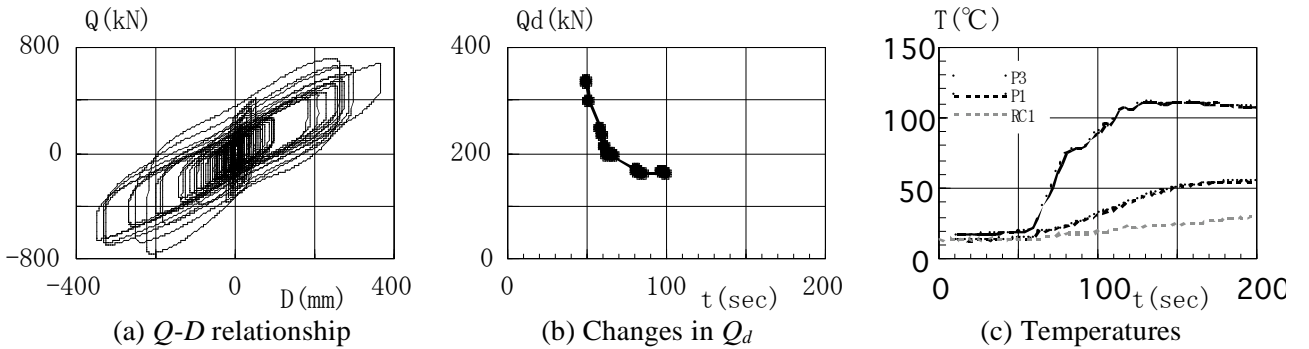


Figure 5. Testing results of earthquake response wave cases (full-scale LRB, Sannomaru waveform)

The inside of the full-scale LRB specimen after all the tests is shown in Photo 1. Little damage was found, the lead slightly bit the upper and lower rubber layers, and plastic deformation remained in the internal steel plate. The total energy input into the specimen was 4.62×10^4 kN.m, which was equivalent to the energy input by the sine wave of $\omega = 100\pi$ rad/s and about 243 cycles.

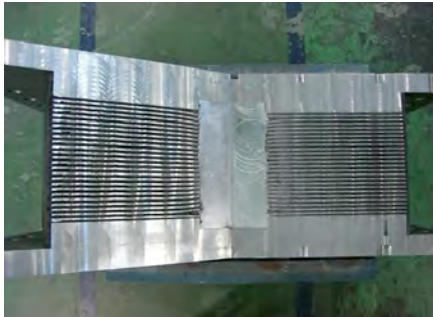


Photo 1. Inside of the full-scale LRB

4 ANALYTICAL METHOD

There are two important points in simulating the heat-mechanics interaction behavior of LRB: to evaluate the temperature rise of the lead plug due to seismic energy absorption, and to simulate the change of the mechanical properties caused by temperature rise. In this section, a heat conduction method is proposed, applying the finite difference method and the relationship between temperature and yield stress of the lead plug.

4.1 Heat conduction analysis

The heat conduction analysis depends on the method by applying the finite difference method. A model used in this analysis in which the LRB, the steel plate attachment and the steel block for the loading test are divided into 26 elements in total shown in Figure 6. For the analysis, upper half part of LRB was modeled considering the symmetry of its shape. It comprises into 5 lead plug elements, 10 laminated rubber elements, 7 steel plate attachment elements, and 4 steel blocks for loading test elements.

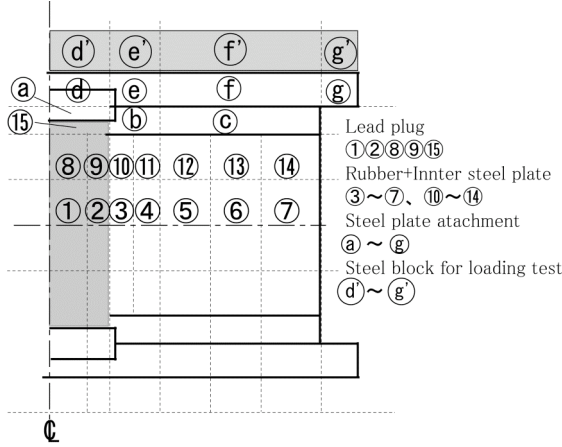


Figure 6. Model for heat conduction analysis

In the heat conduction analysis, temperature θ_{ip} of each element i at step p ($t = p\Delta t$) , is obtained from eq.(4.1) by using the previous step temperature θ_{ip-1} and the temperature increment $\Delta_f\theta_{ip}$ and $\Delta_m\theta_{ip}$.

$$\theta_{ip} = \theta_{ip-1} + \Delta_f\theta_{ip} + \Delta_m\theta_{ip} \quad \text{----- (4.1)}$$

$\Delta_f\theta_{ip}$:temperature increment of element i at step p due to internal heat generation

$\Delta_m\theta_{ip}$: temperature increment of element i at step p due to heat flow

The temperature increment for the lead plug (internal heat generation element) $\Delta_f\theta_{ip}$ is obtained as eq.(4.2.a).

$$\Delta_f\theta_{ip} = \Delta_f E_{ip} / {}_H C_i \quad \text{----- (4.2.a)}$$

$${}_H C_i = V_i \cdot \rho_i \cdot c_i \quad \text{----- (4.2.b)}$$

$\Delta_f E_{ip}$: heat energy generated in element i at step p

${}_H C_i$: heat capacity of element i

V_i : volume of element i

ρ_i : density of element i

c_i : specific heat of element i

The temperature increment of element i caused by the heat transfer is obtained as eq. (4.3).

$$\Delta_m\theta_{ip} = - \sum_j \left\{ \beta_{ij} S_{ij} \lambda_{ij} (\theta_{ip-1} - \theta_{jp-1}) / L_{ij} \right\} {}_H C_i \cdot \Delta t \quad \text{----- (4.3)}$$

S_{ij} : contact area between elements i and j

λ_{ij} : equivalent coefficient of thermal conductivity between elements i and j

L_{ij} : distance between center points of elements i and j

β_{ij} : correction coefficient

Δt : time increment

Finally, the difference equation for heat conduction eq.(4.1) is rewritten as eq. (4.4)

$$\theta_{ip} = \theta_{ip-1} + \Delta_f E_{ip} / {}_H C_i - \sum_j \left\{ \beta_{ij} S_{ij} \lambda_{ij} (\theta_{ip-1} - \theta_{jp-1}) / L_{ij} \right\} {}_H C_i \cdot \Delta t \quad \text{----- (4.4)}$$

4.2 Relationship between temperature and yield stress of lead plug

It is necessary to specify the relationship between the temperature and the yield stress of a lead plug together with the heat conduction analysis to evaluate the effect of the temperature rise of the lead plug on the mechanical property change of the LRB. Here, we propose the eq. (4.5) and Figure 7 based on the simulation analysis for experimental data obtained this time.

The yield stress of lead plug is a function that decreases monotonously with the temperature rise and is set to become 0 in the melting point (T_L) of the pure lead.

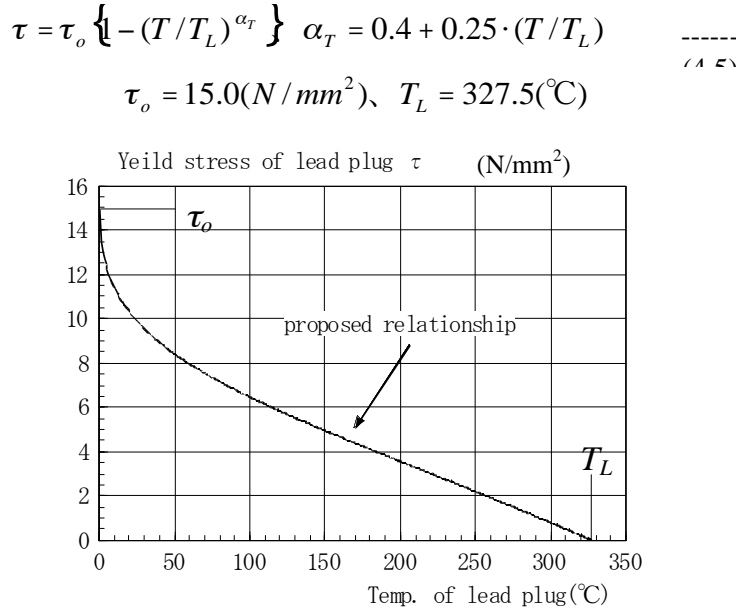
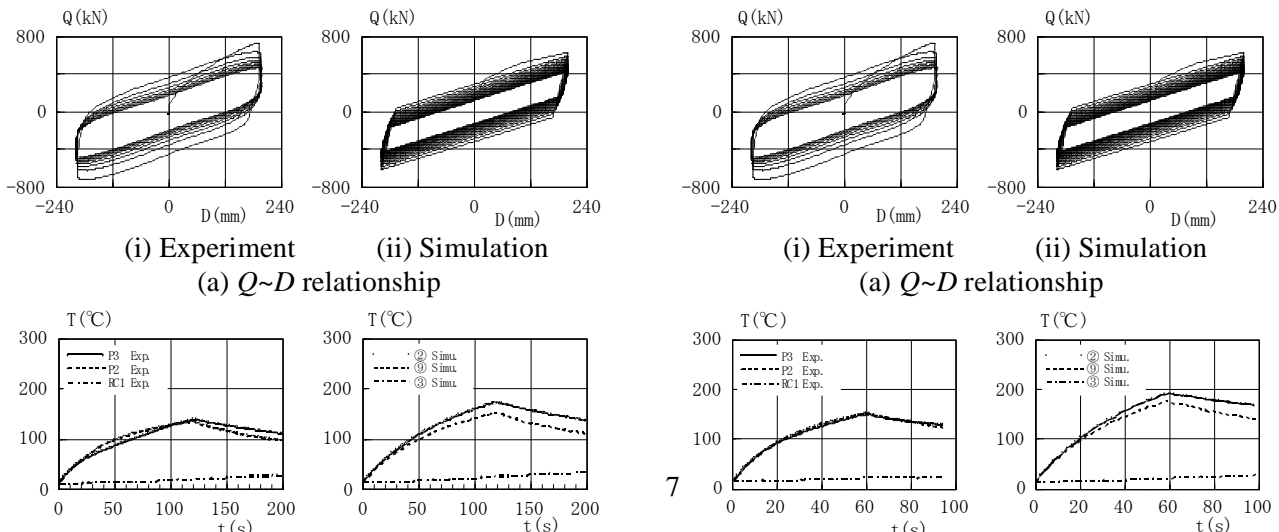
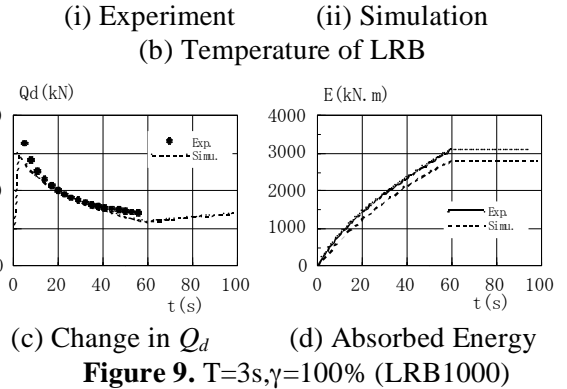
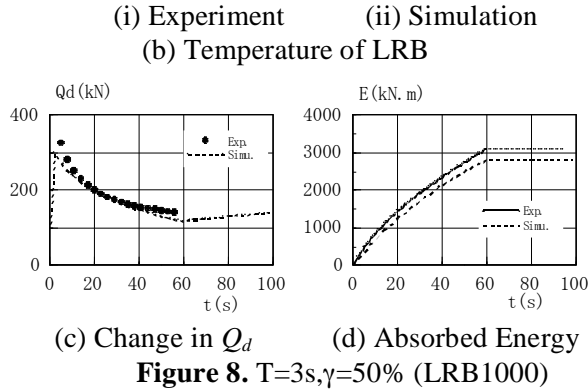


Figure 7. Relationship between temperature and yield stress of lead plug

4.3 Simulation analysis of loading test results

The procedures of the simulation analysis of loading test results is as follows; 1. Input an incremental displacement based on the sinusoidal wave or earthquake wave. 2. Calculate an incremental absorbed energy of the LRB. 3. Evaluate the lead plug temperature considering the heat energy generated in the lead plug and heat flow according to the heat conduction analysis. 4. Evaluate the Q_d of the LRB by applying the eq. (4.5). 5. Set hysteresis loop based on modified bi-linear model with resetting Q_d and turn to 1. During the analysis K_d (rubber stiffness of the LRB) is assumed to stay at the constant value. Figure 8 and Figure 9 show the simulation analysis results for the sinusoidal input of full-scale LRB 1000. In these figures, the relationship of horizontal force and displacement, temperature of LRB, change in Q_d and absorbed energy are shown. According to these figures, both change in mechanical properties and temperatures in the experimental results for the LRB were accurately traced by simulation analysis, thus verifying the validity of our analysis.





4.4 Earthquake response analysis

The development of the earthquake response analysis method considering the effect of LRB temperature rise was basically based on the method described above. The analytical flow is shown in Figure 10. In this method, the heat transfer equation and the vibration equation were solved step by step in parallel.

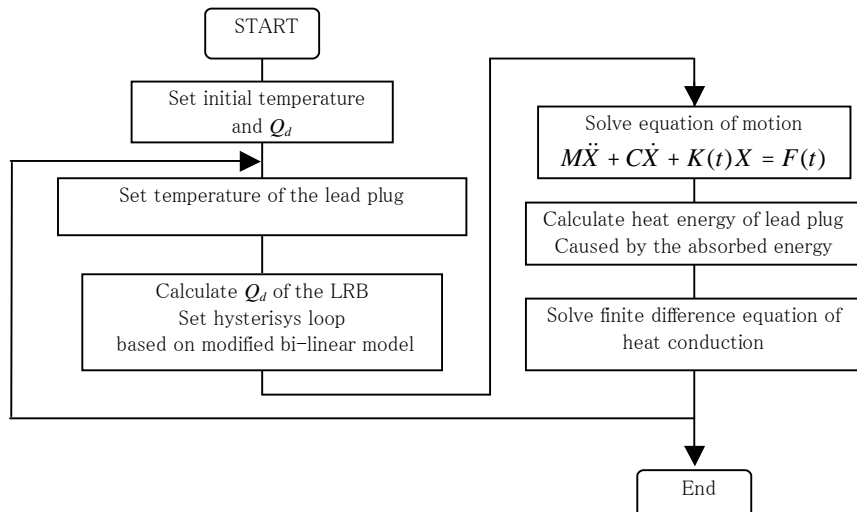


Figure 10. Earthquake response analysis flow

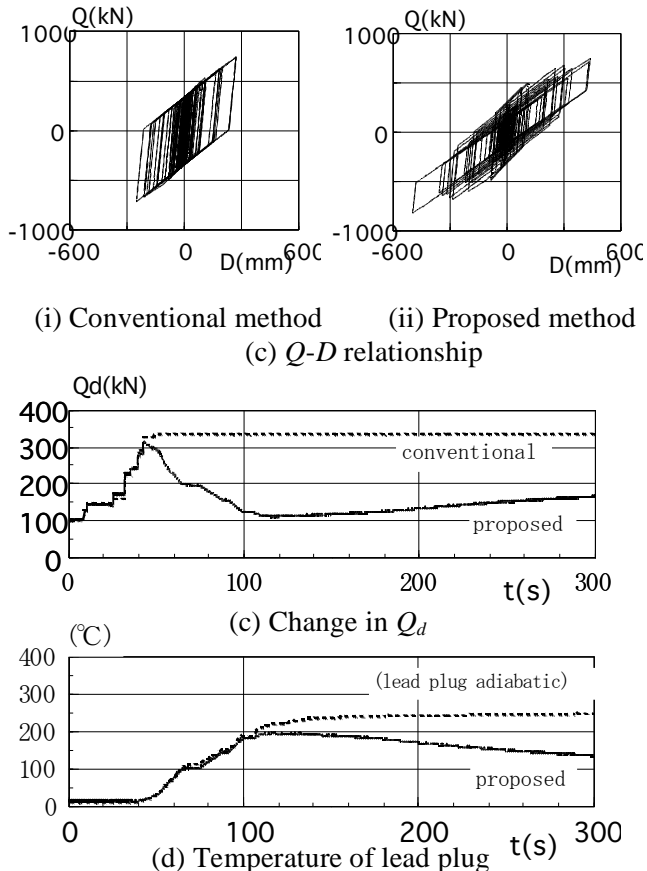
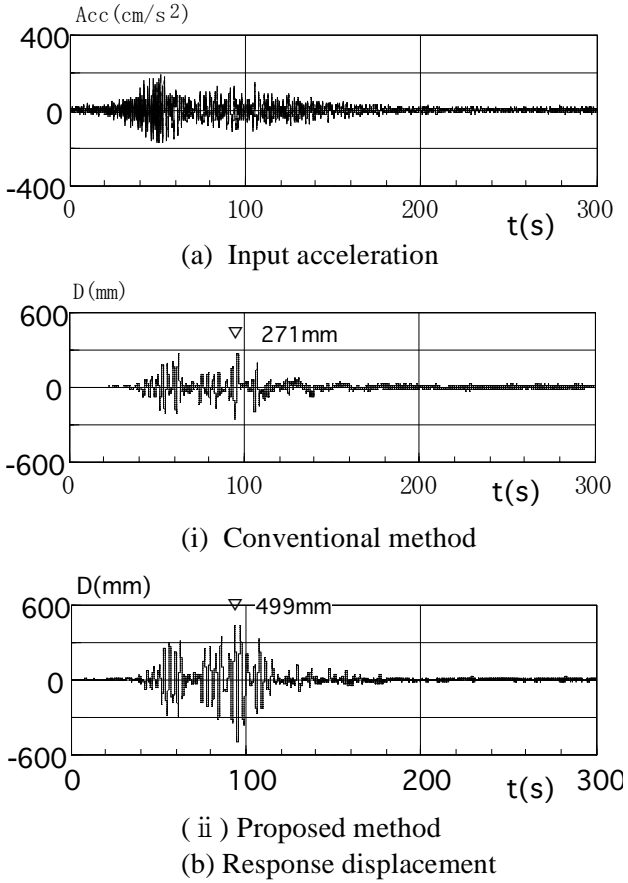


Figure 11. Example of earthquake response analysis
(Nagoya San-no-maru Input, $T_e=2.9s$)

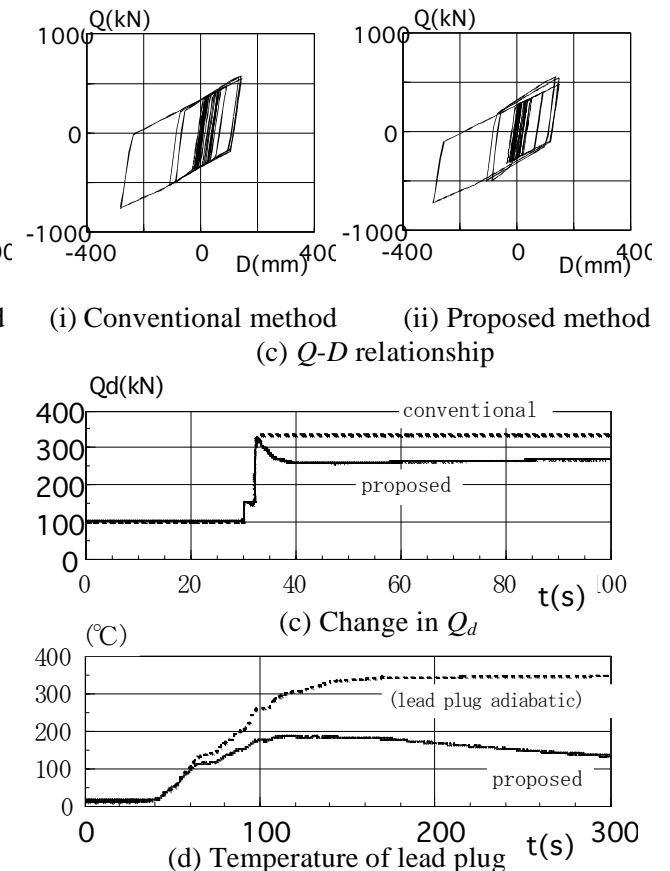
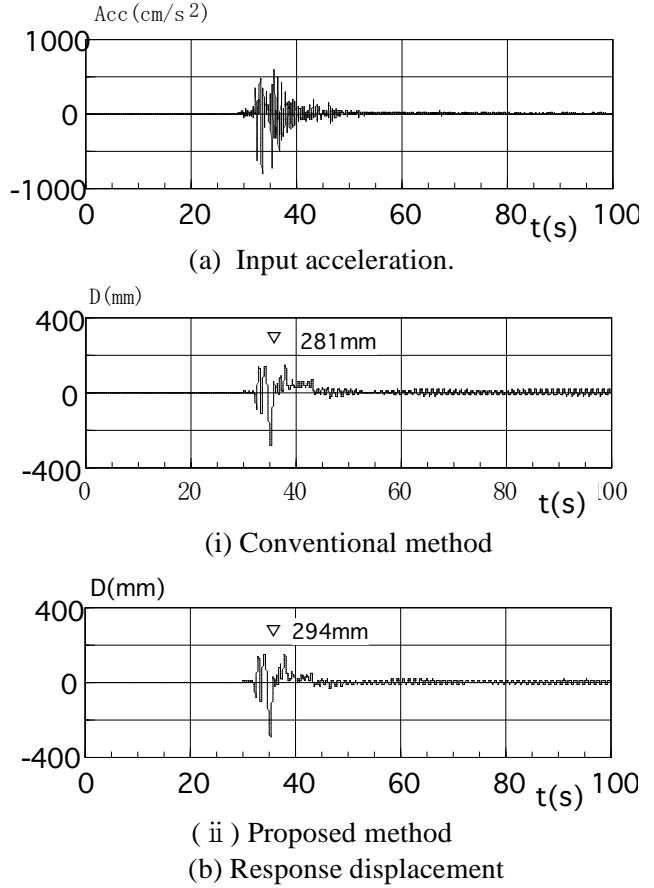


Figure 12. Example of earthquake response analysis
(JMA Kobe(NS) Input, $T_e=2.9s$)

An example of an earthquake response analysis is shown in Figure 11 and Figure 12. The input earthquakes were Nagoya Sannomaru (Figure 11.) and JMA Kobe (Figure 12.). The Nagoya Sannomaru input wave is a

typical long-period artificial strong earthquake ground motion with long principal motion duration. On the other hand, the JMA Kobe input wave, which is an observed ground motion during the Hyogo-ken Nanbu earthquake in 1995, is a typical near-field earthquake with a short duration. When LRB1000 was assumed as a seismic isolator and the axial stress was set as 7.5 N/mm^2 , the earthquake response analysis followed. Equivalent period T_e of at $\omega = 100\%$ becomes 2.9sec. The response values of the conventional and proposed methods were compared. The maximum horizontal displacement for the San-no-maru input was 271 mm for the conventional method, 499 mm for the proposed method, thus showing an increase of 1.84. However, for the JMA Kobe input, the maximum horizontal displacement increase rate was 1.05. It has been understood that the horizontal displacement might become large because of the total input energy and duration time of the seismic ground motion.

5 CONCLUSION

Dynamic loading tests were conducted on lead rubber bearings to confirm the effects of rises in temperature caused by larger and more cyclic deformation on their mechanical properties. The knowledge obtained through this experimental study is as follows:

The yield load of a full-scale LRB specimen with a diameter of 1,000 mm dropped to about 50% at most by a sine wave input, thus far exceeding the energy of an actual seismic motion. However, the rubber stiffness was stable during the tests. The rise in temperature of the lead plug corresponded to the drop in yield load, and the temperature rose to about 150°C . Since the temperature started to rise inside the rubber and flange after the temperature rise in the lead plug, heat generated inside the lead plug was shown to be transmitted to the rubber and steel flange.

Scale effect was observed under a sine wave input. An effect of the temperature rise was larger for full scale LRB than reduced model LRB.

The relationship between the temperature and the yield stress of a lead plug was proposed based on the simulation analysis for experimental data.

An earthquake response analysis method considering the effect of the temperature rise of an LRB was developed based on the simulation analysis of the experiments. According to the proposed response analysis, it is understood that the horizontal displacement might become large under long-period strong earthquakes.

Acknowledgements.

This study was supported by the Japan Society for the Promotion of Science (JSPS) Grant-in-Aid for Scientific Research (B) (No. 18360271, Representative: Y. Takenaka). The San-no-maru waveform was provided by the Chubu Regional Development Bureau, the Aichi Prefecture and a design offices related to the Municipal Hall of Nagoya City.

REFERENCES

- E. Takaoka, Y. Takenaka, A. Kondo, M. Hikita, H. Kitamura (2008), Heat-Mechanics Interaction Behavior of Laminated Rubber Bearings under Large and Cyclic Lateral Deformation, The 14th World Conference on Earthquake Engineering, Oct. 12-17, 2008, Beijing, China
- Takenaka, Y., Kondo, A., et al. (2007). Heat-mechanics interaction behavior of laminated rubber bearings under large and cyclic lateral deformation Part 1~6: Summaries of Technical Papers of Annual Meeting Architectural Institute of Japan B-2, 867-878. (in Japanese)
- Takenaka, Y., Kondo, A., et al. (2008). Heat-mechanics interaction behavior of laminated rubber bearings under large and cyclic lateral deformation Part 9~11: Summaries of Technical Papers of Annual Meeting Architectural Institute of Japan B-2, 397-402. (in Japanese)